

SESSION IV, Papers 1–44

IV-1. The Stiffness of Partially Cracked Brick Walls

D.S. Brooks, G. Sved and D.C. Payne
University of Adelaide, Adelaide, South Australia

ABSTRACT

Brick walls or columns which carry axial loads with eccentricities outside the kern points tend to crack on the bed planes formed by the brick mortar joints. The analysis of these partially cracked walls has previously been based on the assumption that all of the material beyond the uncracked depth can be ignored. This paper examines the true nature of the discrete cracking effect and describes a method of allowing for the tension field stiffening which arises because the bricks remain intact between the cracks in the bed planes. The analysis is based on the finite element method, and a semi-empirical design law is suggested for practical design cases. The calculations are shown to agree closely with experimental results obtained from tests on a series of brick piers and replica steel blocks. It is demonstrated that the tension field stiffening effect may have a significant influence on the load carrying capacity of slender brick walls and columns.

INTRODUCTION

Brick walls or columns which carry axial loads with eccentricities outside the kern points tend to crack on the bed planes formed by the brick mortar joints because the tensile strength of a brick is considerably greater than the flexural bond strength on the brick-mortar interface (Francis¹, Anderson²). The analysis of partially cracked walls has been extensively considered by a number of authors, and Sahlin^{3,4} has presented comprehensive reviews on the various approaches and on the available experimental evidence. In general, the analyses have been based on the assumptions that brickwork cannot sustain any tension stress and that all the material outside the compression zones may be disregarded in evaluating the strength and the stiffness of brick walls. Chapman and Slatford⁵ and Chen⁶ have indicated how the analysis may be extended to deal with a material having only a limited tensile strength, the assumption again being made that all of the material in a cracked zone can be ignored. Chapman and Slatford state that the relatively small and highly variable tensile strength should not be relied upon for design purposes, but Chen and Yokel⁷ have shown that where a small amount of tensile strength exists, it can influence the load deformation characteristics of a wall, particularly if the wall slenderness ratio is high.

An effect which significantly influences the stiffness of a partially cracked wall is the tension stress field in the bricks which remain intact between the cracks in the brick-mortar bed planes. In this investigation of the tension field and its effect on the overall wall stiffness, the bricks and the mortar are treated as linear elastic materials. Both the bricks and mortar are taken to have tensile strengths but the bond strength at the brick-mortar interface is assumed to be zero. These two assumptions are conservative for the design of typical brick-mortar combinations. The latter results in some simplification in the analysis and is justifiable because although the initial bond strength may be significant, once cracking is initiated, it will spread over the entire tension zone. The method of analysis may be extended readily to account for bricks with cores as well as solid bricks.

ANALYSIS

A brick column made up of a series of solid bricks with mortar joints as shown in Figure 1 may be analysed by

considering a number of brickwork units typified by AACC. Each unit comprises two brick halves and a mortar joint, the centre of which is BB (Figure 2). In order to determine the stiffness of the unit AACC the deformations of the brick and mortar components are calculated separately and then combined to obtain the overall deformations of the unit.

In the analysis it is assumed that (by symmetry) plane sections remain plane at the brick half height planes AA and CC. The compressed parts of the interfaces between brick and mortar, DD and EE, are also assumed to remain plane. The deformations of the two half bricks (without the mortar) are shown in Figure 3, together with the finite element mesh used to evaluate this behaviour. Eight noded isoparametric elements were used; plane stress distribution and linear elastic behaviour was assumed, although non-linear analysis can be considered. Nodes along the tensile part of the contact plane DD-EE are uncoupled.

Typical stress distributions are shown in Figure 4 for standard metric bricks (110 mm × 76 mm section), used either "on edge" or "on flat", for an eccentricity of $d/3$. Figure 5 shows in non-dimensional form the relationship between the rotation of the midplanes AA and CC and the load eccentricity for these configurations and also the rotation calculated assuming that the material in the tension zone is fully cracked and hence has no effect on the stiffness.

A similar analysis for a 10 mm mortar joint shows that for both the brick-on-edge and the brick-on-flat construction the rotations for all eccentricities agree to within 1 per cent with those obtained by assuming that all material in the tension zone is fully cracked.

The ratio α of the actual stiffness (allowing for the effect of the tension-zone) to the "fully cracked" stiffness is shown in Figure 6 as a function of the non-dimensional eccentricity ratio e_o/d .

Combining the stiffnesses of the brick and mortar components gives the total flexural stiffness of the unit shown in Figure 2.

If the tension stiffening is ignored, the stress distribution is as shown in Figure 8 and the flexural rigidity (EI product per unit length) of the cracked section is

$$(EI)_{(c)} = E_b \{3(d/2 - e_o)\}^3 / 12 = 9E_b(d/2 - e_o)^3 / 4 \quad (1)$$

where E_b = Young's Modulus for the brick.

The rotation of the brick mid-plane AA with respect to the bearing plane DD-EE shown in Figure 3 is then

$$\begin{aligned}\phi_{b(c)}/2 &= M \cdot (h_b/2)/EI \\ &= P(d/4 - e_o/2) \cdot (h_b/2)/EI_{b(c)} \\ &= (Ph_b/9E_b)(d/2 - e_o)^{-2}\end{aligned}\quad (2)$$

When the effect of tension stiffening is considered, the rotation calculated by the finite element analysis mentioned above can be expressed as

$$\phi_b/2 = (\phi_{b(c)}/2)/\alpha \quad (3)$$

For the mortar, the tension stiffening effect is negligible so that the relative rotation across the mortar joint is

$$\phi_m = (2Ph_m/9E_m)(d/2 - e_o)^{-2} \quad (4)$$

where E_m = Young's Modulus for the mortar.

For the brick-mortar combination, the relative rotation between mid-planes AA and CC of successive bricks (Figure 2) is

$$\phi = \phi_b + \phi_m = (2P/9) \left(\frac{h_b}{\alpha E_b} + \frac{h_m}{E_m} \right) (d/2 - e_o)^{-2} \quad (5)$$

The effective average flexural rigidity of the brick-mortar combination is therefore

$$\begin{aligned}(EI)_{\text{eff}} &= P(d/4 - e_o/2)(h_b + h_m)/\phi \\ &= \frac{9E_b}{4} \left(\frac{d}{2} - e_o \right)^3 \frac{h_b + h_m}{\frac{h_b}{\alpha} + \frac{E_b}{E_m} h_m}\end{aligned}\quad (6)$$

or

$$(EI)_{\text{eff}} = \beta (EI)_{b(c)}, \quad (7)$$

$$\text{where } \beta = (h_b + h_m) / \left(\frac{h_b}{\alpha} + \frac{E_b}{E_m} h_m \right)$$

β is a brickwork stiffening factor which allows for the increase in flexural stiffness over the fully cracked value. Typical variations in β with changes in the eccentricity ratio e_o/d are shown in Figure 7.

EXPERIMENTAL VERIFICATION OF NUMERICAL MODEL

A program of experiments was undertaken to measure accurately both the strain profiles and also the magnitude of the tension field stiffening effect in replica mild steel blocks under eccentric load.

For a check on the strain profiles, a column comprising five steel blocks, each nominally 50 mm × 50 mm × 25 mm, was placed in a testing machine as shown in Figure 9 and loaded eccentrically at each end through machined knife edges. The bearing surfaces of the blocks were precision ground. Electrical resistance strain gauges were fixed to the 50 mm × 50 mm faces of the central steel block as shown in Figure 10. Test eccentricities were $d/5$, $d/3.5$, $d/3$ and the load was applied twice at each eccentricity, once on each

side of the column centre-line. Plots of the experimental and theoretical strain profiles are shown in Figures 12(a), 12(b) and 12(c), the experimental points being the average of two tests. The agreement between computed and experimental strain values was very close.

To measure the tension field stiffening effect, a column of five steel blocks was set up with a pair of Martens mirror extensometers affixed to opposite faces of two alternate blocks as shown in Figure 9. These extensometers enabled the measurement of the relative rotations of the mid-planes of the blocks, the angle of resolution being the order of 5×10^{-5} radians. To define precisely the line of action of the load relative to the blocks in the loaded column, dial gauges were used to measure lateral displacements. Initial alignment of the column was facilitated by lapping the mating surfaces of the blocks, thereby removing any irregularities and enabling intimate contact of the bearing surfaces. The elastic modulus of the steel was determined by tension tests on a solid bar of the same stock material as the blocks, strains being determined by both Martens mirror extensometers and by electrical resistance strain gauges. A comparison of the calculated and experimental values for the brickwork stiffening factor β is given in Table 1 for various load eccentricities. The agreement is within 3 per cent.

TESTS OF BRICK PIERS

A series of six brick piers was tested to check the theoretical stiffness properties of a typical brick and mortar combination. The piers were built in a steel frame to achieve vertical straightness on one face. Each pier comprised six bricks and five mortar joints. All bricks were selected for uniformity and their dimensions were all 228 mm × 108 mm × 75 mm closely. The test set up is as shown in Figure 11.

Six bricks from the batch were each cut to give two sample prisms 75 mm wide × 25 mm thick × 108 mm high which were tested in compression using pairs of 30 mm strain gauges to determine strains. The results for brick elastic modulus are shown in Table 2. The mortar in the piers was 1 cement : 1 lime : 6 sand by volume and the water-cement ratio was 1.41 by weight. Six 25 mm × 25 mm × 50 mm prisms were taken to measure the elastic modulus in compression as for the bricks. The results of initial tangent modulus in uniaxial compression for the mortar prisms are shown in Table 3. All bricks were laid in a saturated surface-dry condition, and in a "brick-on-edge" orientation with 10 mm thick joints. All mortar prisms and brickwork were cured in polythene sheet for 21 days before testing.

Each of the brick piers was tested in a 1000 kN compression machine as shown in Figure 11 and to eliminate problems of material variability, each sample was tested at load eccentricities of $d/6$ and $d/3$, the former value not producing cracking and corresponding therefore to α being equal to 1.0. The loads were applied at each end through pinned joints consisting of steel rollers in machined grooved plates. Rotations at the ends of the piers were measured with bubble micrometers having an accuracy of 2×10^{-5} radians, and a series of dial gauges was used to check the profiles of the deformed shapes. Before testing each pier, an eccentric load was applied to ensure that the mortar joint

interfaces were precracked. This load was not large enough to distress either the bricks or the mortar in the joints.

The dial gauges indicated that the deflected shape of each pier closely approximated a circular curve, and the end rotations computed from the measured deflections agreed with those measured by the bubble micrometers.

The end rotations per unit load for each pier are given in Table 4 for load eccentricities of $d/6$ and $d/3$ together with the ratios of these values. From equation (6) with $h_b = 108$ mm, $h_m = 10$ mm and the corresponding Young's Modulus values given in Tables 2 and 3, the theoretical ratio of the end rotations is 3.08. The average of the experimental values is 2.82 with a coefficient of variation of 3 per cent. Discrepancies between the theoretical and experimental results may be attributed, in part, to residual friction effects in the pin joints through which the load was applied.

APPLICATION TO WALL DESIGN

The curves plotted in Figure 6 from the finite element results can be closely approximated by a continuous surface.

$$\alpha = \alpha\left(\frac{e_o}{d}, \frac{h}{d}\right) = [E_o][R][H]^T \quad (8)$$

$$\text{where } E_o = \left[1 \left(\frac{e_o}{d}\right) \left(\frac{e_o}{d}\right)^2 \left(\frac{e_o}{d}\right)^3 \right]$$

$$\text{and } H = \left[1 \left(\frac{h}{d}\right) \left(\frac{h}{d}\right)^2 \left(\frac{h}{d}\right)^3 \right]$$

and R is a 4×4 matrix of coefficients. By using an orthogonal polynomial approximation to the values of α obtained from the finite element calculations, the R matrix is found to be

$$R = \begin{bmatrix} 1.03 & -1.18 & 0.794 & -0.187 \\ -0.326 & 14.4 & -9.47 & 2.32 \\ 1.22 & -54.1 & 31.3 & -7.98 \\ -1.39 & 61.0 & -18.5 & 4.79 \end{bmatrix} \quad (9)$$

In the ranges $0 \leq \frac{h}{d} \leq 2$, $0.167 \leq \frac{e_o}{d} \leq 0.375$, equations (8) and (9) give values for the stiffening factor α to within 0.5 per cent of the finite element values. Equations (7) and (8) can then be used to determine the flexural stiffness properties of walls under eccentric axial loads. In general, the stiffness of a wall will vary over the entire height wherever the eccentricity of the load exceeds the kern distance, and numerical methods may be used to analyze the wall behaviour under vertical load and to determine the load carrying capacity in either crushing or buckling.⁸

TABLE 1—Brickwork Stiffening Factors

e_o	β Experiment	β Calculated	$\frac{\beta_{\text{Experiment}}}{\beta_{\text{Calculated}}}$
$d/5$	1.01	1.02	0.99
$d/3.5$	1.21	1.22	0.99
$d/3$	1.42	1.47	0.97

CONCLUSIONS

The flexural stiffness of a partially cracked brick wall may be significantly influenced by the tension field effects in the individual bricks. Previous analyses of wall behaviour based on the assumption that the material outside the compression zone can be neglected have resulted in under-estimates for the load carrying capacities of walls. These under-estimates may be particularly significant in the case of walls having slenderness ratios where relatively large flexural deformations occur prior to failure by buckling. In an actual wall, tension field stiffening leads to smaller deformations and hence a greater load carrying capacity in comparison with the corresponding values that would be predicted on the basis of a conventional "no-tension" analysis.

The effect depends upon the eccentricity of the load, the relative stiffnesses of the brick and mortar materials, and the geometrical configuration of the brick-mortar joint arrangement. The degree of stiffening increases with the load eccentricity and is greater for strong mortars having stiffnesses approaching the stiffness of the brick material. Increases in the stiffening effect are also obtained with increases in the height-depth aspect ratio of the bricks.

Numerical representations of the stiffening factors have been presented in this paper for incorporation in the analysis of the structural performance of complete wall systems.

REFERENCES

1. Francis, A.J. "The SAA Brickwork Code: The Research Background", Civ. Eng. Trans., Inst. Eng. Aust., Oct. 1969, Vol. C.E. 11 No. 2, pp. 165-176
2. Anderson, G.W. "Stack-bonded Small Specimens as Design and Construction Criteria", Proc. 2nd International Brick Masonry Conference, Stoke-on-Trent 1970, pp. 38-45
3. Sahlin, S. "Structural Masonry", Prentice-Hall, Inc., New Jersey 1971
4. Sahlin, S. "Discussion on Paper by F.Y. Yokel", Proc. A.S.C.E. ST3, March 1972, pp. 775-776
5. Chapman, J.C. and Slatford, J. "The Elastic Buckling of Brittle Columns", Proc. I.C.E. London, Vol. 6, January 1957, pp. 107-125
6. Chen, W.F. "Discussion on Paper by F.Y. Yokel", Proc. A.S.C.E., ST5, May 1972, pp. 1193-1197
7. Yokel, F.Y. "Stability and Load Capacity of Members with No Tensile Strength", Proc. A.S.C.E., ST7, July 1971, pp. 1913-1926
8. Payne, D.C., Brooks, D.S. and Sved, G. "The Numerical Analysis of Brick Walls and Columns". To be published.

TABLE 2—Young's Modulus for Bricks

Brick Mark	E_b , (GPa)	
	Sample 1	Sample 2
A	9.30	9.87
B	14.40	12.33
C	8.22	8.46
D	7.22	7.79
E	10.05	8.05
F	11.56	9.70

TABLE 3—Young’s Modulus for Mortar

Prism No.	E_m (GPa)
1	7.84
2	7.87
3	8.28
4	8.72
5	8.34
6	8.84

TABLE 4—Experimental Pier Rotations

Pier No.	Relative End Rotation Rate ($\times 10^6$ rad/kN)		Ratio of Rates $e_o(d/3)/e_o(d/6)$
	$e_o = \frac{d}{6}$	$e_o = \frac{d}{3}$	
1	91.6	274	2.99
2	94.6	268	2.83
3	84.6	236	2.79
4	94.2	256	2.72
5	80.8	224	2.77
6	87.0	244	2.80

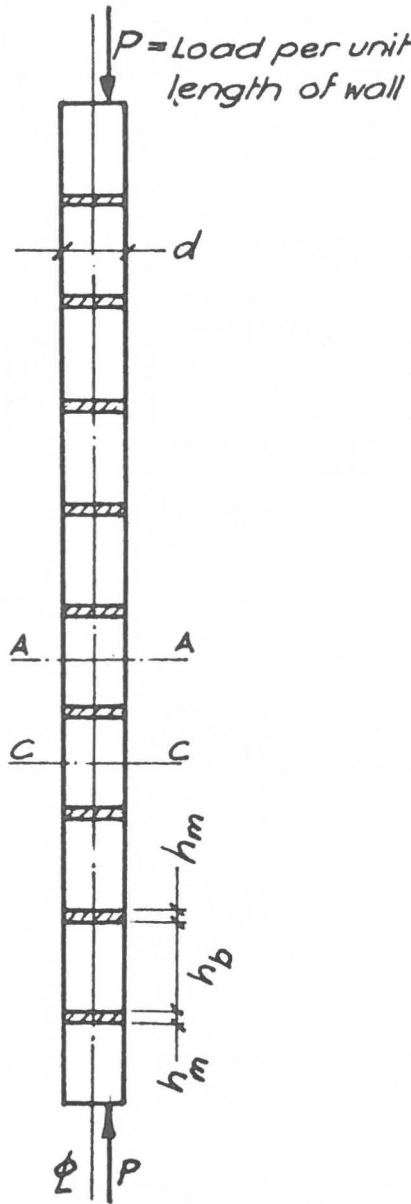


Figure 1.

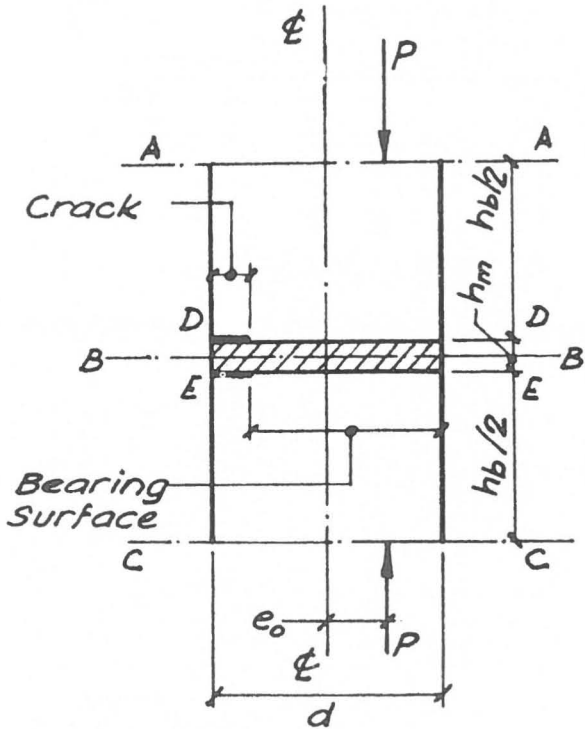


Figure 2. Unit AACC mortar shown hatched

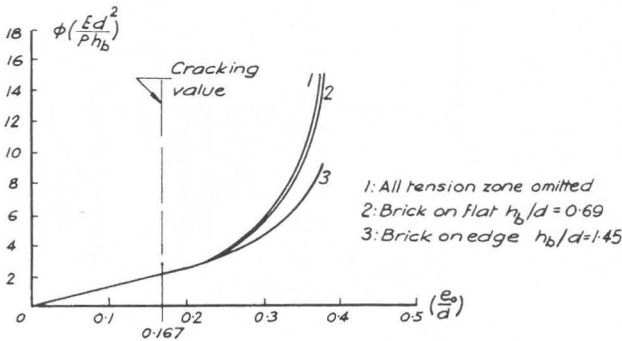


Figure 5.

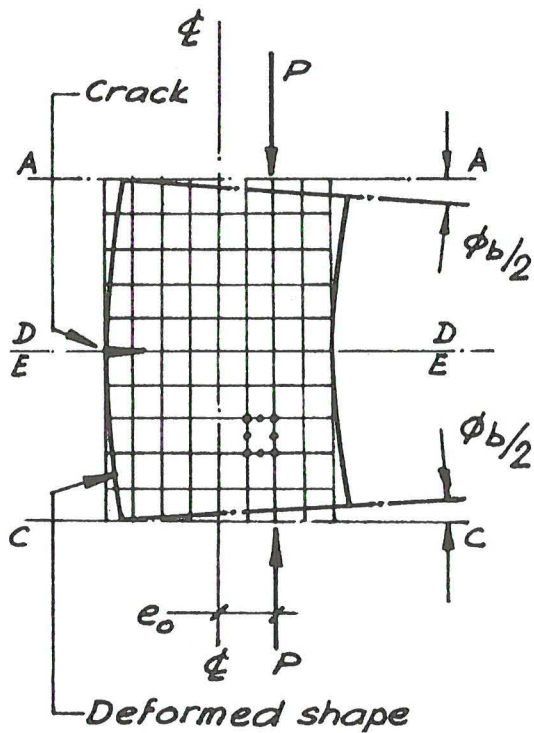


Figure 3. Finite element mesh showing typical element

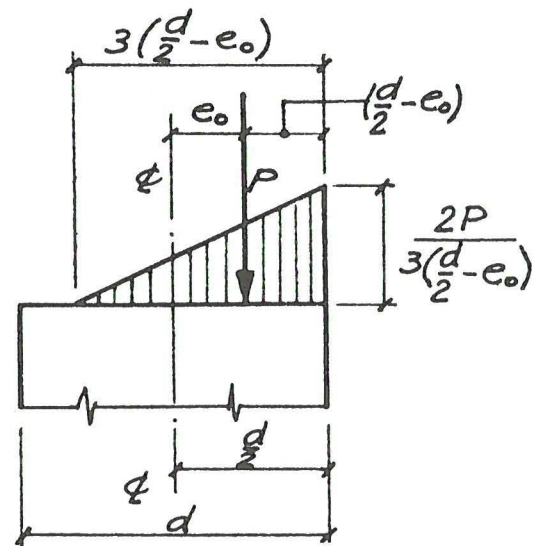


Figure 8. Stress distribution in fully cracked wall

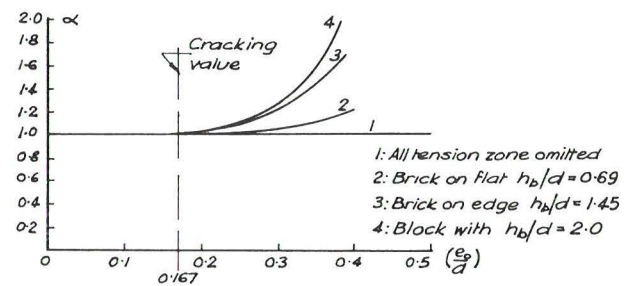
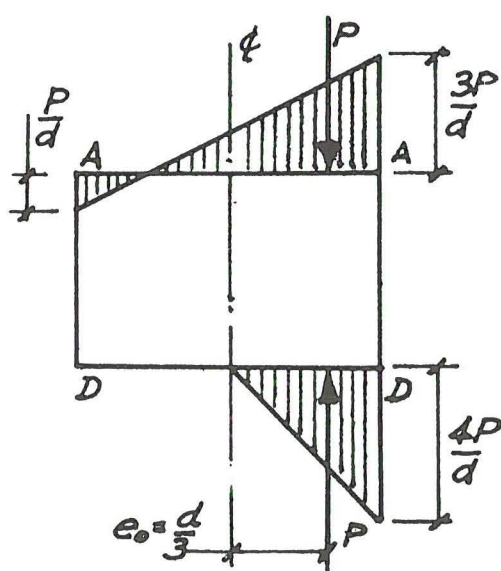
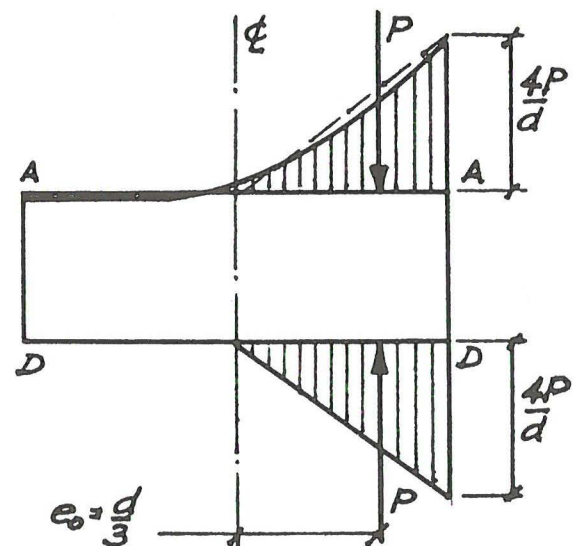


Figure 6.



(a) Brick on edge



(b) Brick on flat

Figure 4. Stress distributions

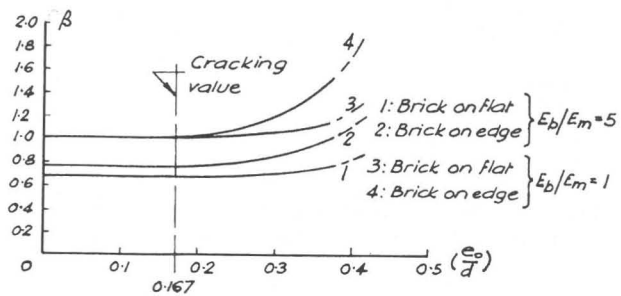
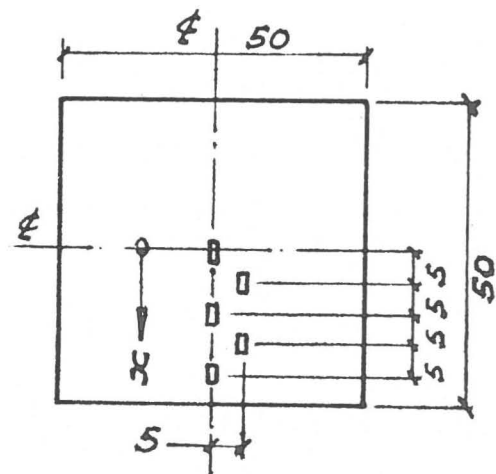


Figure 7.



Location of strain gauges on faces of blocks

Figure 10.

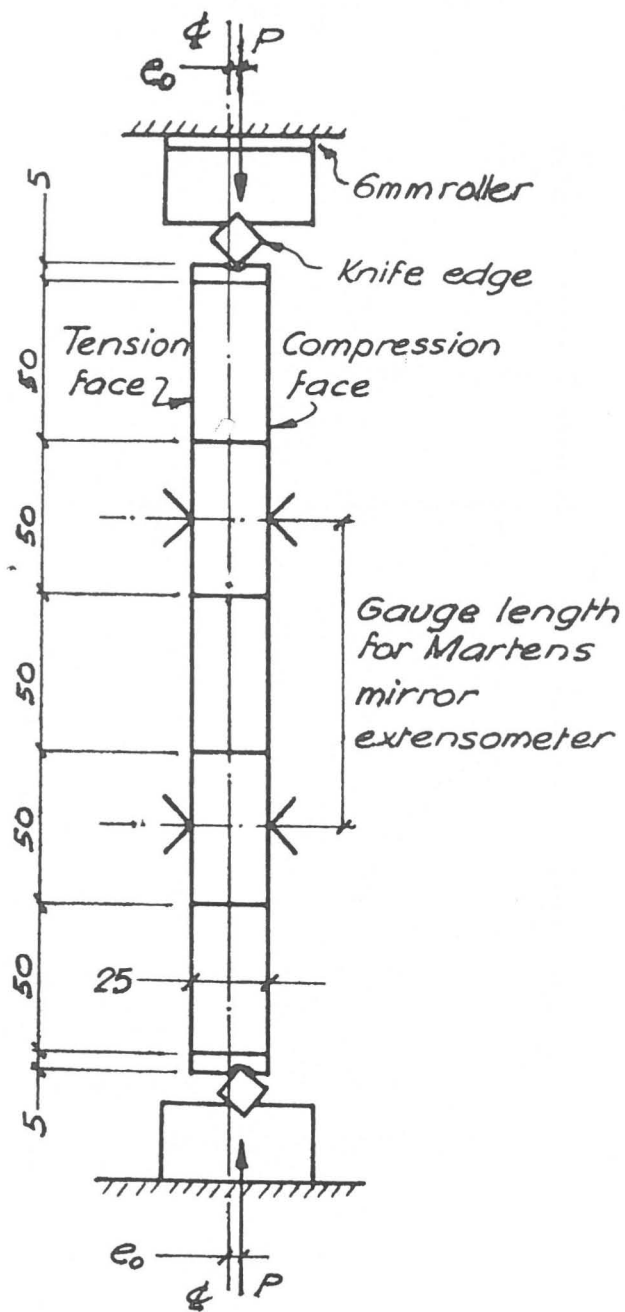


Figure 9.

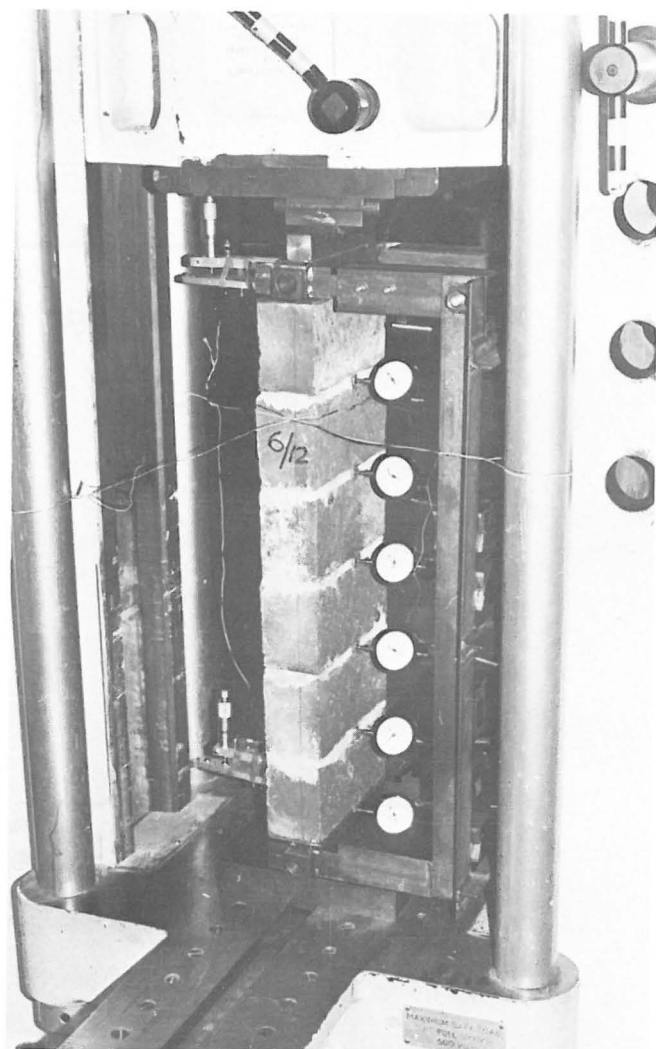


Figure 11.

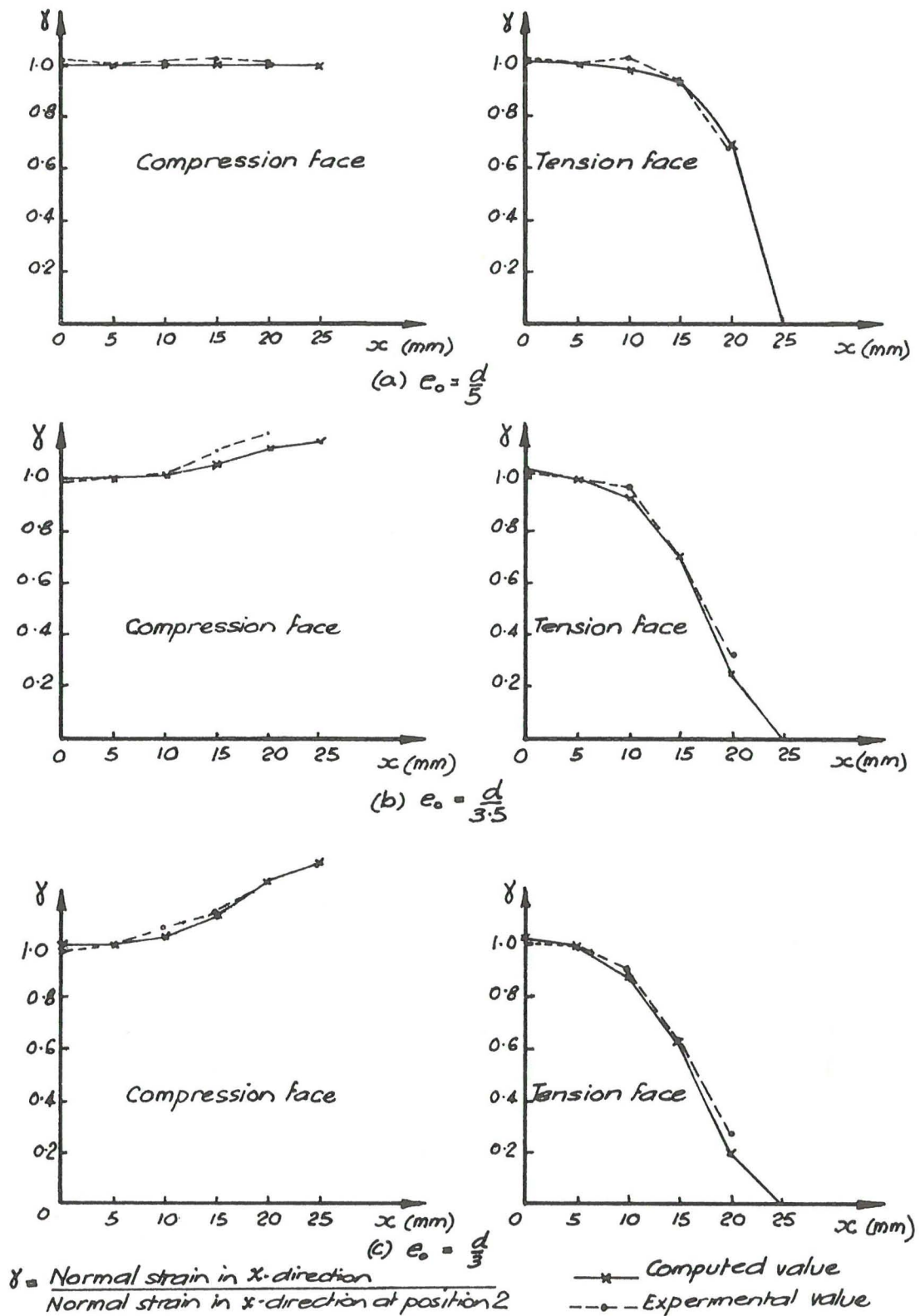


Figure 12. Strain profiles